Computational Materials Science 81 (2014) 184–190

Contents lists available at ScienceDirect

Computational Materials Science

journal homepage: www.elsevier.com/locate/commatsci

Pressure effect on the structural, elastic and electronic properties of Nb_2AC (A = S and In) phases; ab initio study

M. Romeo, R. Escamilla *

Instituto de Investigaciones en Materiales, Universidad Nacional Autónoma de México, Apartado Postal 70-360, México D.F. 04510, Mexico

ARTICLE INFO

Article history:
Received 12 April 2013
Received in revised form 31 July 2013
Accepted 1 August 2013
Available online 6 September 2013

Keywords:
MAX-phases
First-principle
Elastic constants
High pressure

ABSTRACT

The structural parameters, elastic and electronic properties of Nb_2AC (A = S and In) phases were investigated under pressure using first-principles plane-wave pseudopotential density functional theory within the generalized gradient approximation. We find that the effect of pressure on the crystal structure reflects in a compression of the unit cell-volume, mainly along the *c*-axis. On the other hand, the elastic constants, elastic modulus and the Debye temperature θ_D increase monotonically as the pressure increases. The relationship between brittleness and ductility shows that Nb_2AC are brittle at 0 GPa and only the Nb_2SC phase tended to be ductile under pressure from 4 GPa to 10 GPa. Finally, we find that the density of states at the Fermi level decrease in the Nb_2InC phase and increase in Nb_2SC phase under pressure.

1. Introduction

Ternary carbides and nitrides with the chemical formula $M_{n+1}AX_n$ present a new class of solids [1]. MAX phases are made up of an early transition metal (M), an A-group element of the periodic table, and either carbon or nitrogen (X), the subscript in changing from 1 to 3 [1]. Most of these phases were synthesized by Nowotny and co-workers in the sixties [2]. For these last years, the efforts of characterization of MAX phases, have shown interesting and unusual set of properties of these materials [3–5]; generally they present a good thermal and electrical conductivity, machinable, with exceptional resistance to thermal shock, are good oxidation resistant, quite stiff and relatively light [1,3–5].

In the family of carbines, only seven low-temperature superconducting materials have been discovered: Mo_2GaC (T_c = 4 K [6]), Nb_2SC (T_c = 5 K [7]), Nb_2SnC (T_c = 7.8 K [8]), Nb_2AsC (T_c = 2 K [9]), Ti_2InC (T_c = 3 K [10]), Nb_2InC (T_c = 7.5 K [11]) and Ti_2GeC (T_c = 9.5 K [12]). Let us note that for the majority of the other MAX phases experimental or theoretical researches of their superconductivity are still absent.

Few experimental and theoretical works have been done to investigate the structural, elastic and electronic properties of Nb_2AC with A = S and In under pressure. Recent studies on Nb_2SnC under pressure [13] shows that the structural parameter (*z*) shifts with pressure and thus presents a different variation mechanism from that of the other hexagonal lattice with a similar structure. The shift of the Nb atom along the *c*-axis might also contribute to the stiffness of the *c*-axis. On the other hand, it also shows that the density of states (DOS) at the Fermi level decreases with increasing pressure, due to the decrease of the contribution of Nb 4d states at the Fermi level.

In the present paper, we would like to deepen our understanding of this system Nb_2AC (A = S and In) under pressure by the determination of their structural, elastic, electronic properties, using first-principles plane-wave pseudopotential density functional theory within the generalized gradient approximation (GGA).

2. Methods of calculation

In this work we have carried out a serie of calculations based on the CASTEP (Cambridge Serial Total Energy Package) code [14,15], which built on the density functional theory (DFT) [16], the interaction between valence electron and core electron was treated under the pseudopotential approximation and the plan wave approach (PP-PW) [17]. Exchange–correlation energy was estimated within Perdew–Wang functional (PW91) [18]. First-principles electronic structure calculations may be performed with sufficient accuracy to resolve energy differences as small as a few meV per atom. Total energy is the main quantity in first principal calculations [14], we have used the BFGS (Broyden–Fletcher–Goldfarb–Shanno) algorithm [19] to find the lowest energy of the crystal with an energy tolerance of 10^{-6} eV/atom. First Brillouin zone was sampling on $9 \times 9 \times 8$ irreducible *k* points [20]. We employ the norm conserving pseudopotential model [21], with a cut off energy 360 eV. Careful convergence tests show that with these

* Corresponding author. Tel.: +52 5 622 4635; fax: +52 5 616 1251.
E-mail address: rauleg@unam.mx (R. Escamilla).

0927-0256/$ - see front matter © 2013 Elsevier B.V. All rights reserved.
http://dx.doi.org/10.1016/j.commatsci.2013.08.010

Table 1
Summary of calculated structural parameters (a, c, c/a, z and V) phases at zero pressure for the Nb_2AC (A = S and In), compared with available previous experiment and other theoretical results.

Phase	Methods	a (Å)	c (Å)	c/a	z	V (Å^3)	Reference
Nb_2SC	GGA PW91	3.307	11.642	3.521	0.0949	110.25	This work
	Exp.	3.294	11.553	3.507	0.0964	108.56	[7]
	FLAPW-GGA	3.3204	11.7093	3.527	0.0952	111.80	[22]
	FLAPW-GGA	3.2942	11.7835	3.577	0.096		[23]
	GGA-PBE	3.290	11.670	3.550	0.0956		[24]
	GGA-PW91	3.312	11.65	3.517			[27]
Nb_2InC	GGA-PW91	3.185	14.546	4.567	0.0822	127.79	This work
	Exp.	3.172	14.37	4.530			[11]
	FLAPW-GGA	3.1933	14.4952	4.5392	0.0821	128.01	[22]
	GGA-PW91	3.1889	14.4703	4.537	0.0827		[25]
	LDA CA-PZ	3.137	14.280	4.552	0.0830		[26]
	GGA-PW91	3.196	14.47	4.527			[27]

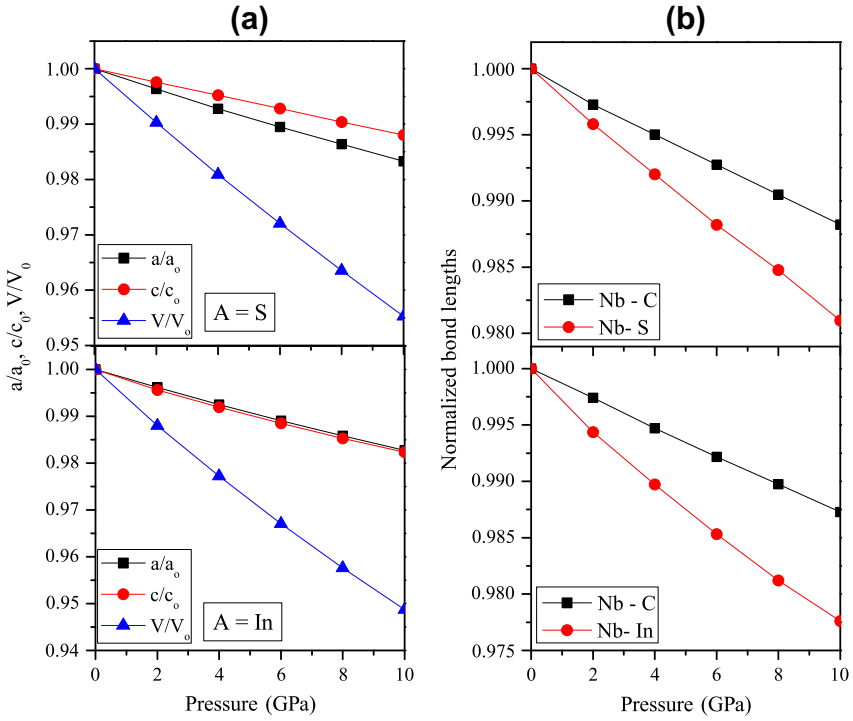

Fig. 1. (a) The normalized a/a_0, c/c_0 and volume V/V_0 as a function of pressure at $T = 0$. (b) Variation of the normalized bond lengths between the atoms with pressure.

parameters, the convergence of the total energy calculations is guaranteed. The convergence tolerances were set as follows: 0.002 eV/Å for the maximum force on atoms, 10^{-4} Å for the maximum atomic displacement, and 0.003 for the maximum strain amplitude.

3. Geometry and structure optimization

The considered superconducting Nb_2AC (A = S and In) phases possess the hexagonal structure with a space group $P6_3/mmc$ (No. 194), where blocks of transition metal carbides [NbC] (formed by edge-shared Nb_6C octahedron) are sandwiched with A atomic sheets. The Wyckoff positions of atoms are C: 2a (0, 0, 0), A: 2d (1/3, 2/3, 3/4), and Nb atoms: 4f (1/3, 2/3, z), where z is 0.09493 and 0.0807 for A = S [7] and In [11], respectively.

Firstly, all the structures Nb_2AC (A = S and In) were optimized for each pressure value up to 10 GPa, with respect to internal parameters z, energy, force, stress, and displacement (see Table 1). In Fig. 1a, we exhibit the pressure dependence of the normalized lattice parameters a/a_0, c/c_0 and volume V/V_0 (where a_0, c_0, and V_0 are the structural parameters at 0 GPa). The normalized bond lengths r_1/r_{10} and r_2/r_{20} (where r_{10} and r_{20} are the bond lengths of Nb–A = S, In and Nb–C at 0 GPa, respectively) are shown in Fig. 1b.

We notice in Fig. 1a that, when pressure increases from 0 to 10 GPa, the compressibility along the c-axis increase from S to In; as a consequence, the curve of r_1/r_{10} becomes steeper than the corresponding one of the r_2/r_{20}, indicating that the direction along Nb–A (A = S and In) is more easily compressed. Moreover, according to Fig. 1b, we can also observe that the stiffness of Nb–C bonds essentially unchanged for A = S and In. Therefore, the atoms in the interlayers become closer, and the interactions between them become stronger; contractions of Nb–A and Nb–C bond lengths under pressure result in the change of bonding anisotropy of Nb_2AC structure, which induces the variety of electronic structure.

4. Elastic stiffness tensor calculation

Several methods are available for computation of elastic constants, but currently the finite strain method seems to be most commonly used, and this one is used in the present work. In this approach, the ground-state structure is strained according to symmetry-dependent strain patterns with varying amplitudes and a subsequent computing of the stress tensor after a reoptimization of the internal structure parameters, i.e., after a geometry optimization with fixed cell parameters. The elastic constants are then the proportionality coefficients relating the applied strain to the computed stress, $\sigma = C_{ij}\varepsilon_j$.

From the optimized structure of the Nb_2AC (A = S and In) phases under pressure we have calculated the fifth independent elastic constants C_{11}, C_{12}, C_{13}, C_{33}, C_{44}, which allowed us to obtain the bulk K and shear G moduli (see Fig. 2a). Usually, for such calculations, two main approximations are used, namely the Voigt (V) [28] and Reuss (R) [29] schemes.

Thus, in terms of the Voigt approximation, these moduli are:

$$G_V = \frac{1}{30}(C_{11} + C_{12} + 2C_{33} - 4C_{13} + 12C_{44} + 12C_{66}) \quad (1)$$

$$K_V = \frac{1}{9}[2(C_{11} + C_{12}) + C_{33} + 4C_{13}]. \quad (2)$$

In terms of the Reuss approximation:

$$G_R = \frac{\frac{5}{2}\{C_{44}C_{66}[C_{33}(C_{11} + C_{12}) - 2C_{13}^2]\}}{3K_VC_{44}C_{66} + (C_{44} + C_{66})[C_{33}(C_{11} + C_{12}) - 2C_{13}^2]} \quad (3)$$

$$K_R = \frac{C_{33}(C_{11} + C_{12}) - 2C_{13}^2}{C_{11} + C_{12} + 2C_{33} - 4C_{13}}. \quad (4)$$

For estimations of elastic parameters for polycrystalline materials, Hill's approximation [30] is widely used, where the actual effective moduli for polycrystals are expressed as the arithmetic mean of the two above-mentioned limits – Voigt and Reuss: $G = \frac{1}{2}(G_R + G_V)$ for shear moduli and $K = \frac{1}{2}(K_R + K_V)$ for bulk moduli, (see Fig. 2b).

Using these values, Young's modulus (E) and Poisson's ratio (v), can be obtained by

$$E = \frac{9KG}{3K + G} \quad (5)$$

and

$$v = \frac{3K - 2G}{2(3K + G)}. \quad (6)$$

To evaluate the mechanical anisotropy we using the bulk modulus along the a and c-axes (K_a and K_c), respectively as [31].

$$K_a = \frac{\Lambda}{2 + \alpha} \quad (7)$$

$$K_c = \frac{\Lambda}{2\alpha + \alpha^2} \quad (8)$$

$$\Lambda = 2(C_{11} + C_{12}) + 4C_{13}\alpha + C_{33}\alpha^2 \quad (9)$$

$$\alpha = \frac{C_{11} + C_{12} - 2C_{13}}{C_{33} - C_{13}}. \quad (10)$$

On the other hand, we calculate its anisotropies in compression and shear,[32] respectively, as

$$A_{comp} = 100\frac{K_V - K_R}{K_V + K_R} \quad (11)$$

and

$$A_{shear} = 100\frac{G_V - G_R}{G_V + G_R} \quad (12)$$

The above elastic parameters presented in Table 2 allow us to make the following conclusions: (i) The C_{ij} constants for Nb_2AC phases are positive and increase monotonically under pressure; and satisfy the generalized criteria [33] for mechanically stable crystals: $C_{44} > 0$, $C_{11} > |C_{12}|$, and $(C_{11} + C_{12})\,C_{33} > 2C_{13}^2$. (ii). From Table 2 is observed that the Nb_2SC phase (200.1 GPa) has a bulk modulus (K) higher than the Nb_2InC phase (156.4 GPa); in turn, in both phases the shear moduli (G) are similar: 100.3 for Nb_2SC and 101.1 for Nb_2InC. Thus, for the considered phases $K > G$; this implies that the parameter limiting the mechanical stability of these materials is the shear modulus. (iii). According to Pugh's criteria [34], a material should behave in a ductile manner if $G/K < 0.5$, otherwise it should be brittle. For 0 GPa, $(Nb_2SC)_{G/K} = 0.50 < (Nb_2InC)_{G/K} = 0.65$;

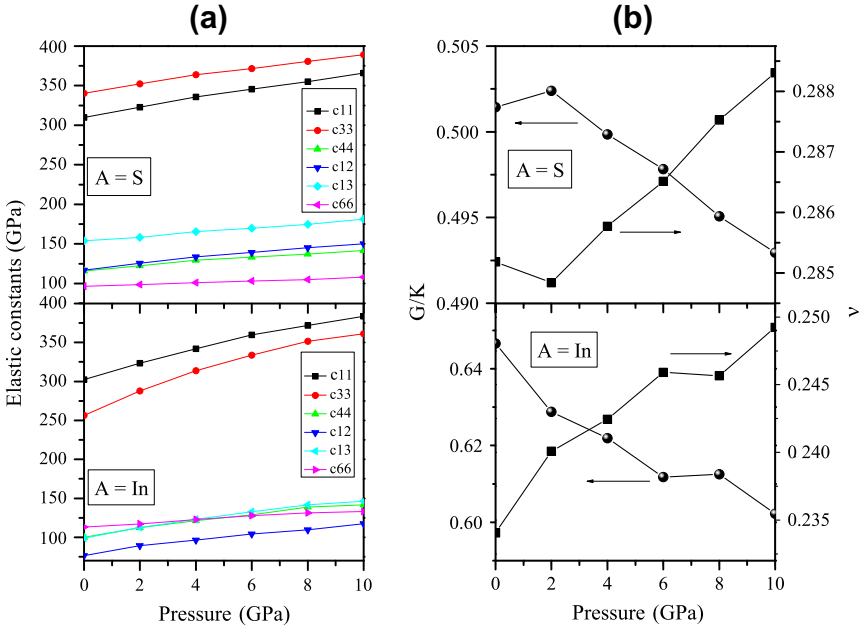

Fig. 2. (a) Elastic constants and (b) variation of the G/K and Poisson ratio (v) for the Nb_2AC (A = S and In) phases in function of pressure.

Table 2
Elastic constants (C_{ij}), bulk modulus (K, in GPa), shear modulus (G, in GPa), Young modulus (E, in GPa) and Poisson's ratio (v) of Nb_2AC (A = S, In) at 0 GPa.

Phase	C_{11}	C_{12}	C_{13}	C_{33}	C_{44}	K	G	E	v	Reference
Nb_2SC	309.9	116.9	154.0	340.5	115.8	200.1	100.3	257.9	0.285	This work
	303.6	116.9	155.1	315.7	88.1	220.9	88.6	234.5	0.323	[22]
	320.1	100.8	152.5	327.2	125.2	196.8	107.7	273.2	0.270	[24]
	309.0	106.0	159.0	310.0	118.0	197.0	101.0	258.0		[27]
Nb_2InC	302.5	76.3	98.8	256.3	100.1	156.4	101.1	249.6	0.234	This work
	291.0	77.0	118.0	289.0	57.0	182.4	79.6	208.5	0.309	[22]
	286.9	74.1	107.3	265.1	104.0					[25]
	363.0	103.0	131.0	306.0	148.0	187.0				[26]
	291.0	76.0	108.0	267.0	102.0	159.0	99.0	247.0		[27]

Table 3
Mechanical anisotropy (K_a, K_c) and anisotropies in compression and shear (A_{comp}, A_{shear}) of Nb_2AC (A = S, In) at 0 GPa.

Phase	K_a	K_c	A_{comp}	A_{shear}	Reference
Nb_2SC	524.9	824.0	0.52	0.97	This work
	527.0	767.4			[22]
	522.1	786.9			[24]
	517.1	805.0			[27]
Nb_2InC	492.5	428.0	0.08	0.67	This work
	459.1	594.7			[22]
	460.5	496.4			[25]
	469.6	494.4			[27]

Table 4
Debye temperature (θ_D), Grüneisen constant (γ) and unit cell-volume (Å^3) of Nb_2SC and Nb_2InC phases at 0 GPa.

Phase	θ_D	γ	V (Å^3)	Reference
Nb_2SC	502.7	1.82	110.30	This work
	540.0		109.39	[24]
Nb_2InC	454.8	1.61	127.40	This work
	457.1	1.64	127.44	[25]
	515.0		121.70	[26]

i.e. according to this indicator the Nb_2AC phases will behave in a brittle manner; however, when the pressure increases from 4 to 10 GPa, the Nb_2SC phase tended to be ductile (see Fig. 2b). (See Tables 3 and 4)

An additional argument for the variation in the brittle/ductile behavior of Nb_2AC phases follow from the Poisson ratio v. Indeed, for brittle materials, these values are small enough, whereas for ductile metallic materials, v is typically 0.33. In this work, the Poisson ratio v calculated from 0 GPa to 10 GPa behaves as: $(Nb_2SC)_v = (0.285–0.288) > (Nb_2InC)_v = (0.234–0.249)$; for the pressure range studied, the Nb_2AC phases will behave in a brittle manner (see Fig. 2b).

On the other hand, for determine the types of chemical bond, we using the typical relation between bulk and shear modulus (G/K): for covalent and ionic materials, the values are $G/K \approx 1.1$ K and $G/K \approx 0.6$ K, respectively. In our cases, G/K values change from 0.50 to 0.49 for Nb_2SC and from 0.64 to 0.60 for Nb_2InC. The previous results suggest that the ionic bonding is important in the Nb_2AC compounds.

Fig. 3a shows the mechanical anisotropy K_a and K_c values against pressure. We observed clearly that K_a and K_c increased linearly in the pressure range studied. In the Nb_2SC phase, $K_c > K_a$ from 0 GPa to 10 GPa; whereas for the Nb_2InC phase $K_a > K_c$ for pressures lower than 5 GPa and $K_c > K_a$ for pressures higher than 5 GPa. The larger K_c at high pressure is consistent with the stiffness of c-axis. Fig. 3b shows the elastic anisotropy, it is observed that while the value of A_{comp} decrease in both phases; the value of A_{shear} increases in the Nb_2SC phase and decrease in Nb_2InC under pressure. Obviously, the Nb_2AC phases are isotropic in compression and in shear, but the degree of isotropy decreases with pressure.

As an important fundamental parameter, the Debye temperature (θ_D) is closely related to many physical properties of solids such as the specific heat and the melting temperature. One of the standard methods to calculate the Debye temperature is from elastic constants data, since θ_D may be estimated from the average sound velocity (v_m), by the following equation [35],

$$\theta_D = \frac{h}{k}\left[\frac{3n}{4\pi}\left(\frac{N_A\rho}{M}\right)\right]^{1/3} v_m, \tag{13}$$

where h is Plank's constant, k is Boltzmann's constant, N_A is Avogadro's number, ρ is the density, M is the molecular weight and n is the number of atoms in the molecule. The average sound velocity v_m is given by

$$v_m = \left[\frac{1}{3}\left(\frac{2}{v_t^3} + \frac{1}{v_l^3}\right)\right]^{-1/3}, \tag{14}$$

where v_l and v_t are the longitudinal and transverse elastic wave velocities, respectively, which are obtained from Navier's equations as follows [36]:

$$v_l = \sqrt{\frac{3K + 4G}{3\rho}} \tag{15}$$

and

$$v_t = \sqrt{\frac{G}{\rho}}, \tag{16}$$

where ρ is the density, K is the bulk modulus and G is the shear modulus.

Application of the hydrostatic pressure not only decreases the interatomic distances in a solid. Since the force constants of the crystal lattice modes are also changed with pressure, the corresponding phonon frequencies will be modified as well. This effect can be quantified by the so-called Grüneisen constant γ, which shows how the phonon frequencies (and, eventually, Debye temperature (θ_D)) vary with volume V of the crystal; it is defined as follows [37].

$$\gamma = -\frac{dln\theta_D}{dlnV}. \tag{17}$$

As Eq. (17) implies, estimations of the (θ_D) values require the knowledge of the volume dependence of the Debye temperature, which can be easily obtained from the results of the crystal lattice optimization and elastic constants calculations under pressure.

Fig. 4a shows that the Debye temperature increases linearly with pressure; the pressure coefficient of 3.61 and 4.41 K/GPa for Nb_2SC and Nb_2InC, respectively. The volume-coefficients of the

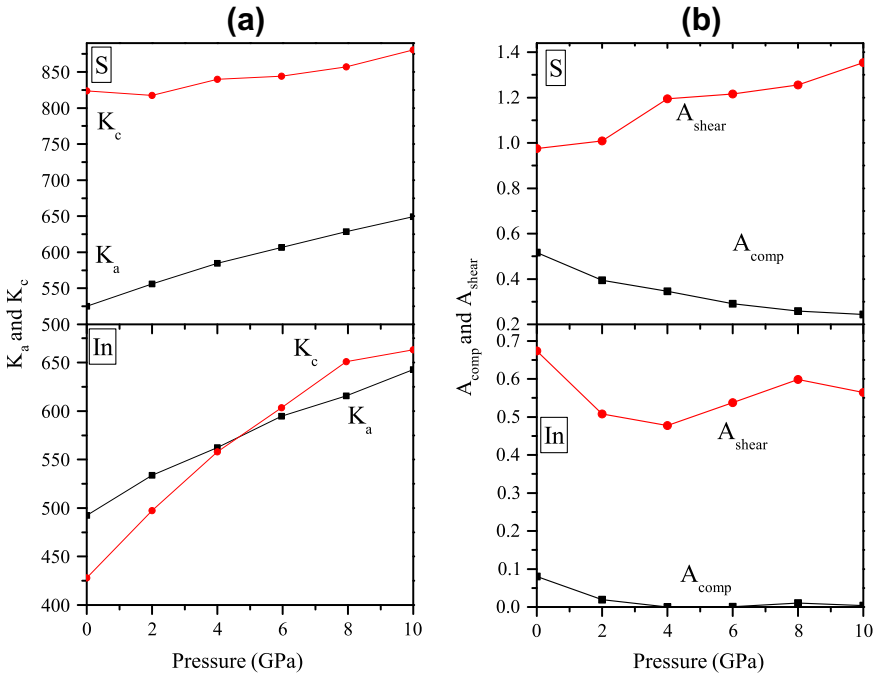

Fig. 3. (a) Variation of the bulk modulus K_a and K_c along the a- and c-axis and (b) variation of the anisotropies in compression and shear with pressure.

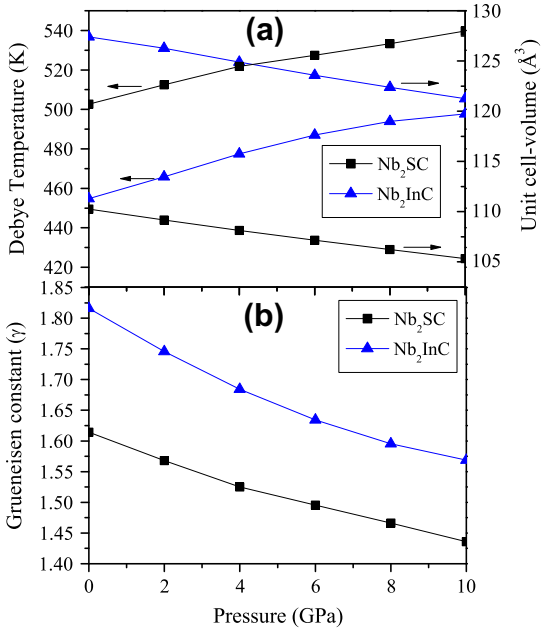

Fig. 4. (a) Debye temperature θ_D – unit cell volume and (b) Grü neisen parameter (γ) of the Nb_2AC compounds under pressure.

Debye temperature estimated from the linear approximation of data in Fig. 4a are −7.36 (Nb_2SC) and −6.44 K/Å^3 (Nb_2InC). These values, together with the calculated values of the Debye temperature and volume, were used in Eq. (17). The calculated values of the Grüneisen parameter vs pressure are given in Fig. 4b. At the ambient pressure $\gamma = 1.61$ (Nb_2SC) and 1.82 (Nb_2InC); with increasing pressure γ decreases non-linearly, as shown in the same figure. Such a decrease of γ can be related to increased values of the elastic constants with pressure and somewhat weakened dependence of the vibrational frequencies on volume (or pressure); all these factors arise from the anharmonic effects.

5. Electronic and bonding properties under pressure

Finally, the effects of pressure on the density of states (DOS) of Nb_2AC (A = S and In) are examined, for pressures varying within the range from zero to 10 GPa. Fig. 5a displays the pressure dependence at $P = 0$ and 10 GPa of the total (DOS) and partial density of states (PDOS) of Nb_2AC phases near the Fermi level, (vertical line is the Fermi level (E_F)). The calculated equilibrium density of states at the Fermi level (E_F) at 0 GPa were 3.29 and 3.42 electrons/eV for Nb_2SC and Nb_2InC, respectively. The comparison of the density of states at the Fermi level (E_F) at 0 GPa of Nb_2SC with those reported by others, show us that our value is similar to the calculated by Nasir and Islam (3.54 states/eV) [24], while the of Nb_2InC is close to obtain by Shein and Ivanovskii (3.62 states/eV)[38].

The local feature of the DOS curve around the Fermi-level (E_F) is a reasonable indicator of the intrinsic stability of a crystal. A local minimum at E_F implies higher structural stability because it signifies a barrier for electrons below the E_F ($E < 0$ eV) to move into unoccupied empty states ($E > 0$ eV); whereas a local maximum at E_F is usually a sign of structural instability. This semi-quantitative criterion works reasonably well for the results of Fig. 5a. Nb_2SC and Nb_2InC have a local minimum at E_F, suggesting a higher level of stability. These facts correlate quite well with the observation that these phases are easier to synthesize.

From Fig. 5a we observed that at 0 GPa, the Nb 4d states dominate at Fermi level and should contribute to the conduction in the Nb_2AC phases. The contributions between −8.0 to −3.0 and −7.0 to −3.0 eV can be associate to the C 2p states of the Nb_2SC and Nb_2InC phases, respectively. We observed that the C 2p states had the same shape as the 4d electronic states of Nb atoms located between C layers. It is indicative of a hybridization between Nb 4d and C 2p states and thus of a covalent interaction.

On the other hand, is observed that the In 5p states and the S 3p interact with the Nb 4d states within the energy range from −4.0 to −1.0 and from −8.0 to −5.0, respectively. Since the In 5p–Nb 4d hybrids are lower in energy that the S 3p–Nb 4d hybrid's ones suggesting that Nb–S bonds are stronger than Nb–In bonds (see Fig. 1a). Comparing the previous hybrid's with the C 2p–Nb 4d

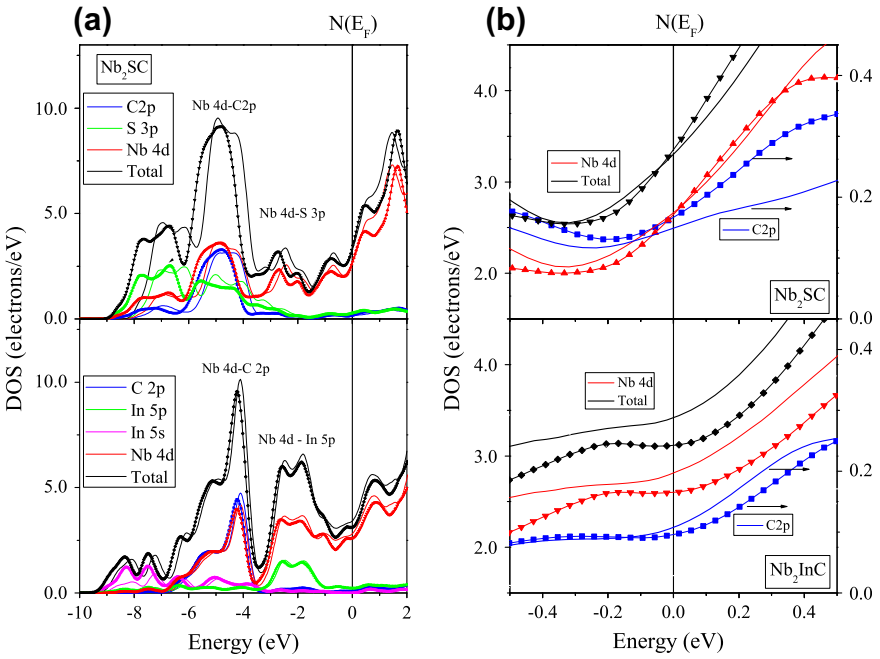

Fig. 5. (a) The total and the partial DOS of Nb_2AC at 0 GPa (continuous line) and 10 GPa (line + symbol) and (b) zoom from −0.50 to 0.50 eV.

hybrids, we observed that the Nb–C bonds are stronger than Nb–In or Nb–S bonds (see Fig. 1b). It is this strong C 2p–Nb 4d hybridization, which stabilizes the structure of Nb_2AC (A = S and In) a general trend in MAX phases. In addition, the above mentioned covalent Nb–C and Nb–A bonds, the metallic-like Nb–Nb bonding occurs owing to the overlap of the near Fermi level Nd 4d states; whereas the ionic contribution is due to the difference in electronegativity between the compressing elements: Nb (1.60), C (2.55), S (2.58) and In (1.78).

In Fig. 5b, we observed in the Nb_2InC phase a decrease in the DOS $N_{Nb}(E_F)$ and the DOS $N_C(E_F)$ associated with the niobium and carbon states at the Fermi level, respectively as pressure increases. Whereas in the Nb_2SC phase is observed only an increase in the DOS $N_C(E_F)$ associated to carbon states at the Fermi level. The rest of contributions remains virtually unchanged. As a consequence, at 10 GPa the density of states at the Fermi level E_F decreases in the Nb_2InC phase, similar to one observed in Nb_2SnC and MgB_2 [13,39] and increases in the Nb_2SC phase. The DOS at the Fermi level is an important parameter known to affect the superconducting transition temperature T_c. Judging from Bardeen–Cooper–Schrieffer superconducting theory, the reduction of the density of states at the Fermi level shows that the transition temperature T_c decrease as pressure increases [40].

6. Conclusions

In summary, the structural, elastic and electronic properties of the Nb_2AC (A = S and In) phases under pressure have been investigated using planewave pseudopotential density functional theory within the generalized gradient approximation (GGA). We find that the effect of pressure on the crystal structure reflects in a compression of the unit cell-volume, more easily along the *c*-axis than on the *a*-axis. We also observed that the elastic constants and elastic modulus increase monotonically. As a consequence, the hardness and the compression of the phases increase under pressure. Debye temperature θ_D was calculated and found that it increases under pressure. According to the results of our calculations, an increase in the pressure would lead to a decrease in the density of states (DOS) of Nb_2InC phase due, mainly to the decrease of the DOS $N_{Nb}(E_F)$ and the DOS $N_C(E_F)$ associated with the niobium and carbon states at the Fermi level, respectively; and increase in Nb_2SC phase due, mainly to the increase of the DOS $N_C(E_F)$ associated to carbon states at the Fermi level.

Acknowledgments

The authors thanks to the Project DGAPA-UNAM IN-102412/24 and for their technical help to R. Gomez, F. Silvar, C. González and J. Morales.

References

[1] M.W. Barsoum, Prog. Solid State Chem. 28 (2000) 201.
[2] V.H. Nowtony, Prog. Solid State Chem. 5 (1971) 27.
[3] M.W. Barsoum, Physical Properties of the MAX Phases, Encyclopaedia of Materials: Science and Technology, Elsevier, Amsterdam, 2006.
[4] M.W. Barsoum, M. Radovic, Mechanical Properties of MAX Phases, Encyclopedia of Materials: Science and Technology, Elsevier, Amsterdam, 2004.
[5] M.W. Barsoum, T. El-Raghy, Am. Sci. 89 (2001) 334.
[6] L.E. Toth, J. Less, Common Met. 13 (1967) 129.
[7] K. Sakamaki, H. Wada, H. Nozaki, Y. Onuki, M. Kawai, Solid State Commun. 112 (1999) 323.
[8] A.D. Bortolozo, O.H. Sant-Anna, M.S. da Luz, C.A.M. dos Santos, A.S. Pereira, K.S. Trentin, A.J.S. Machado, Solid State Commun. 139 (2006) 57.
[9] S.E. Lofland, J.D. Hettinger, T. Meehan, A. Bryan, P. Finkel, S. Gupta, M.W. Barsoum, G. Hug, Phys. Rev. B 74 (2006) 174501.
[10] A.D. Bortolozo, O.H. Sant-Anna, C.A.M. dos Santos, A.J.S. Machado, Solid State Commun. 144 (2007) 419.
[11] A.D. Bortolozo, Z. Fisk, O.H. Sant-Anna, C.A.M. dos Santos, A.J.S. Machado, Physica C 469 (2009) 256.
[12] A.D. Bortolozo, O.H. Sant'Anna, C.A.M. dos Santos, A.J.S. Machado, Mater. Sci. Poland 30 (2012) 2.
[13] M. Romero, R. Escamilla, Comput. Mater. Sci. 55 (2012) 142.
[14] S.J. Clark, M.D. Segall, C.J. Pickard, P.J. Hasnip, M.J. Probert, K. Refson, M.C. Payne, Z. Kristallogr. 220 (2005) 220.
[15] M.D. Segall, P.J.D. Lindan, M.J. Probert, C.J. Pickard, P.J. Hasnip, S.J. Clark, M.C. Payne, J. Phys.Condens. Matter 14 (2002) 2717.
[16] W. Kohn, L.J. Sham, Phys. Rev. A 140 (1965) 1133.
[17] M.C. Payne, M.P. Teter, D.C. Allan, T.A. Arias, J.D.J. Joannopoulos, Rev. Mod. Phys. 64 (1992) 1045.
[18] J.P. Perdew, J.A. Chevary, S.H. Vosko, K.A. Jackson, M.R. Pederson, D.J. Snigh, C. Fiolhais, Phys. Rev. B 46 (1992) 6671.

[19] T. Pfrommer, G.M. Cote, S.G. Louie, M.L. Cohen, J. Comput. Phys. 131 (1997) 133.
[20] H.J. Monkhorst, J.D. Pack, Phys. Rev. B 13 (1976) 5188.
[21] D.R. Hamann, M. Schluter, C. Chiang, Phys. Rev. Lett. 43 (1979) 1494.
[22] I.R. Shein, A.L. Ivanovskii, Phys. Status Solidi B 248 (2011) 228.
[23] I.R. Shein, V.G. Bamburov, A.L. Ivanovskii, Doklady Phys. Chem. 411 (2006) 317.
[24] M.T. Nasir, A.K.M.A. Islam, Comput. Mater. Sci. 65 (2012) 365.
[25] M.G. Brik, N.M. Avram, C.N. Avram, Comput. Mater. Sci. 63 (2012) 227.
[26] A. Bouhemandou, Mod. Phys. Lett. B 22 (2008) 2063.
[27] M.F. Cover, O. Warschkow, M.M.M. Bilek, D.R. McKenzie, J. Phys.: Condens. Matter 21 (2009) 305403.
[28] W. Voigt, Leipzig 739 (1928).
[29] A. Reuss, Z. Angew, Math. Mech. 9 (1929) 49.
[30] R. Hill, Proc. Phys. Soc. 65 (1952) 349.
[31] A.S. Sikder, F. N, A.K.M.A. Islam, Phys. Lett. A 350 (2006) 288.
[32] D.H. Chung, W.R. Buessem, F.W. Vahldiek, in: S.A. Mersol (Ed.), Anisotropy in Single Crystal Refractory Compounds, Plenum, New York, 1968, p. 217.
[33] M. Born, Proc. Cambridge Philos. Soc. 36 (1940) 160.
[34] S.F. Pugh, Philos. Mag. 45 (1954) 833.
[35] O.L. Anderson, Phys. Chem. Solids 24 (1963) 909.
[36] E. Schreiber, O.L. Anderson, N. Soga, Elastic Constants and their Measurements, McGraw-Hill, New York, 1973.
[37] J.P. Poirier, Introduction to the Physics of the Earths Interior, Cambridge University Press, 2000.
[38] I.R. Shein, A. Ivanovskii, JETP Lett. 91 (2010) 410.
[39] F.N. Islam, A.K.M. A Islam, M.N.J. Islam, Phys.: Condens. Matter 13 (2001) 11661.
[40] J. Bardeen, L.N. Cooper, J.R. Schrieffer, Phys. Rev. 108 (1957) 1175.